Keiji Tanigaki,[1] Ken L. Chambliss,[1] Ivan S. Yuhanna,[1] Anastasia Sacharidou,[1] Mohamed Ahmed,[1] Dmitriy N. Atochin,[2] Paul L. Huang,[2] Philip W. Shaul,[1] and Chieko Mineo[1]

Endothelial Fcγ Receptor IIB Activation Blunts Insulin Delivery to Skeletal Muscle to Cause Insulin Resistance in Mice

PATHOPHYSIOLOGY

Modest elevations in C-reactive protein (CRP) are associated with type 2 diabetes. We previously revealed in mice that increased CRP causes insulin resistance and mice globally deficient in the CRP receptor Fcγ receptor IIB (FcγRIIB) were protected from the disorder. FcγRIIB is expressed in numerous cell types including endothelium and B lymphocytes. Here we investigated how endothelial FcγRIIB influences glucose homeostasis, using mice with elevated CRP expressing or lacking endothelial FcγRIIB. Whereas increased CRP caused insulin resistance in mice expressing endothelial FcγRIIB, mice deficient in the endothelial receptor were protected. The insulin resistance with endothelial FcγRIIB activation was due to impaired skeletal muscle glucose uptake caused by attenuated insulin delivery, and it was associated with blunted endothelial nitric oxide synthase (eNOS) activation in skeletal muscle. In culture, CRP suppressed endothelial cell insulin transcytosis via FcγRIIB activation and eNOS antagonism. Furthermore, in knock-in mice harboring constitutively active eNOS, elevated CRP did not invoke insulin resistance. Collectively these findings reveal that by inhibiting eNOS, endothelial FcγRIIB activation by CRP blunts insulin delivery to skeletal muscle to cause insulin resistance. Thus, a series of mechanisms in endothelium that impairs insulin movement has been identified that may contribute to type 2 diabetes pathogenesis.

Fcγ receptors (FcRs) are receptors for IgG that classically regulate processes in immune response cells including B cells, T cells, dendritic cells, and monocytes (1). FcRs are categorized into activating receptors (Fcγ receptor [FcγR]I, FcγRIIA, and FcγRIII) and inhibitory receptors, with the latter group consisting of a single subtype, FcγRIIB (1,2). In addition to IgG, the pentraxins C-reactive protein (CRP) and serum amyloid P component are ligands for FcR (3–6). Prompted by numerous studies in humans demonstrating an association between a modest elevation in CRP and type 2 diabetes (7–10), we previously determined how CRP impacts glucose homeostasis in CRP transgenic mice (TG-CRP) and wild-type mice administered CRP (11). We discovered that an increase in CRP causes insulin resistance that is due to attenuated skeletal muscle glucose disposal. The abnormality in glucose homeostasis caused by CRP did not occur in FcγRIIB$^{-/-}$ mice globally deficient in the receptor, linking FcγRIIB to metabolic health and disease for the first time. However, considering that FcγRIIB is expressed in numerous cell types including B lymphocytes, which modulate insulin sensitivity through multiple mechanisms (12,13), the cellular context in which the receptor negatively impacts glucose homeostasis and how it does so are currently unclear. A greater understanding of the processes by which FcγRIIB potentially contributes to type 2 diabetes may reveal new targets for prophylactic or therapeutic interventions for the disease.

We previously discovered that FcγRIIB is expressed in endothelial cells, including the endothelium in skeletal muscle microvasculature (5,11,14). Since the endothelium participates in the regulation of skeletal muscle glucose disposal (15), in the present work we tested the hypothesis that the activation of endothelial FcγRIIB by CRP negatively

[1]Center for Pulmonary and Vascular Biology, Department of Pediatrics, University of Texas Southwestern Medical Center, Dallas, TX
[2]Cardiovascular Research Center and Cardiology Division, Department of Medicine, Massachusetts General Hospital and Harvard Medical School, Boston, MA

Corresponding authors: Chieko Mineo, chieko.mineo@utsouthwestern.edu, and Philip W. Shaul, philip.shaul@utsouthwestern.edu.

influences glucose homeostasis. Mechanisms in endothelium are critically involved in insulin transport from the circulation to skeletal muscle myocytes, with insulin undergoing transcytosis across the endothelium in a process that is rate limiting for peripheral insulin action (16–20). Cell culture studies have shown that the transcytosis requires insulin signaling (21,22) and that it is stimulated by nitric oxide (NO) (23), and we previously demonstrated that FcγRIIB activation by its ligands such as CRP inhibits endothelial NO synthase (eNOS) activation by various stimuli, including insulin (14,24). We therefore tested the additional hypotheses that endothelial FcγRIIB activation by CRP blunts skeletal muscle insulin delivery and that the adverse effect of FcγRIIB activation on glucose homeostasis can be negated by the maintenance of NO bioavailability.

RESEARCH DESIGN AND METHODS

Generation and Characterization of Study Mice

The targeting construct to create floxed FcγRIIB mice (FcγRIIB$^{fl/fl}$) contained loxP sites inserted in intron 1 and intron 3, and the heterozygous fcgr2b$^{fl/+}$ mice created were backcrossed to C57BL/6 mice for more than eight generations. In recognition that FcγRIIB is abundant in B cells, FACS analysis was performed on spleen-derived B cells (positive for CD45R) to assess receptor expression. FcγRIIB abundance in B cells from FcγRIIB$^{fl/fl}$ was similar to that in FcγRIIB$^{+/+}$, indicating that the floxed mouse is not hypomorphic (Supplementary Fig. 1B, C, and F), and B cells from FcγRIIB$^{fl/fl}$:CAG-Cre displayed minimal expression of FcγRIIB similar to that in cells from FcγRIIB$^{-/-}$ mice (Supplementary Fig. 1D and E), indicating effective Cre excision.

Mice with endothelial cell–specific deletion of FcγRIIB were generated by crossing FcγRIIB$^{fl/fl}$ with vascular endothelial cadherin promoter-driven Cre mice (VECad-Cre) (C57BL/6 background) (25). These mice were further crossed with TG-CRP mice on C57BL/6 background (11,26,27) to yield mice with elevated CRP and normal versus deficient FcγRIIB in endothelial cells (FcγRIIB$^{fl/fl}$:TG-CRP or FcγRIIB$^{fl/fl}$:VECad-Cre:TG-CRP, respectively). In our prior work, glucose intolerance and insulin resistance were observed in TG-CRP mice, with CRP levels of 3–14 μg/mL (11). In the current project CRP elevation was modestly greater, approaching 20–24 μg/mL (Fig. 2A), but this does not impact the key question posed, which is whether there is a loss of the metabolic effects of CRP by endothelial deletion of FcγRIIB. The role of eNOS antagonism in CRP-induced insulin resistance was evaluated by crossing TG-CRP with mice expressing a point mutation in eNOS Ser^{1176} that yields a constitutively active enzyme that cannot be inhibited by Ser^{1176} dephosphorylation (S1176D) (28,29).

For evaluation of the efficiency and cell specificity of FcγRIIB deletion from endothelial cells in vivo, primary endothelial cells were isolated from mouse aorta as previously described (30), spleen-derived B cells were studied as described above, and myeloid lineage cells were purified from bone marrow using biotinylated rat anti-mouse Mac-1 antibody (BD Biosciences), streptavidin particles (BD

Biosciences), and Easysep kits (STEMCELL Technologies). Cell type–specific marker expression was evaluated by flow cytometer using fluorescein isothiocyanate (FITC)-conjugated rat anti-mouse CD16/CD32 antibody (1 μg/mL; FcγRIIB, BD Biosciences), Alexa Fluor 647–conjugated monoclonal anti-CD45R antibody (1 μg/mL; B cell–specific marker, eBioscience), Alexa Fluor 647–conjugated rat anti-mouse CD31 (0.4 μg/mL; PECAM1 [endothelial cell–specific marker], BD Biosciences), or Alexa Fluor 647–conjugated rat anti-mouse Ly-6G/Ly-6c antibody (1 μg/mL; myeloid lineage cell–specific marker, BD Biosciences). The care and use of all study animals were approved by the Institutional Animal Care and Use Committee at the University of Texas Southwestern Medical Center.

Evaluation of Adiposity

Body weight was measured, and fat mass and lean body mass were determined by nuclear magnetic resonance (Minispec NMR Analyzer; Bruker) (31).

Evaluation of Glucose Homeostasis

Glucose tolerance tests (GTTs) and insulin tolerance tests (ITTs) were performed in male mice at 10–13 weeks of age. After fasting for 4–6 h, the mice received an injection with D-glucose (1 g/kg body wt i.p.) or insulin (1 unit/kg body wt i.p.) (11). Tail vein blood samples were obtained at the indicated times for plasma glucose measurement by glucometer (OneTouch Ultra2, Johnson & Johnson). Fasting plasma insulin concentrations were determined by ELISA (category no. 90080, version 15; Crystal Chem) (31). HOMA of insulin resistance (HOMA-IR) was calculated to assess differences in insulin sensitivity (32).

### Skeletal Muscle Glucose Uptake, Insulin Delivery, and Insulin Signaling

Skeletal muscle glucose uptake was measured as previously reported (11,33). For simultaneous assessment of insulin delivery to the skeletal muscle, insulin action on eNOS in skeletal muscle microvasculature, and skeletal muscle insulin signaling when the signaling response is maximal (34), experiments were performed using nonlabeled bovine insulin. Fasted mice received tail vein injections with vehicle (saline) or insulin (1 unit/kg body wt); 5 min later the soleus and gastrocnemius were harvested without perfusion and homogenized in PBS, and the homogenates were prepared for protein determination, insulin measurement by ELISA (Crystal Chem), and immunoblotting. The ELISA used detects both mouse and bovine insulin, with 2.1-fold greater sensitivity for bovine versus mouse insulin. Phosphorylated eNOS and total eNOS, phosphorylated insulin receptor (IR) and total IR, and phosphorylated Akt and total Akt were detected by immunoblotting using anti–phospho-eNOS (S1177 for human, S1176 for mouse; Cell Signaling Technology), anti-eNOS (Cell Signaling Technology), anti–phospho-IRβ (Y1120/1151; Cell Signaling Technology), anti-IRβ (Santa Cruz Biotechnology), anti–phospho-Akt (S473; Cell Signaling Technology); and anti-Akt (Cell Signaling Technology) antibodies.

Endothelial Cell Insulin Uptake and Transcytosis

Primary bovine aortic endothelial cells (BAECs) were obtained as previously described (24) and human aortic endothelial cells (HAECs) were purchased from Lonza, and cells were used within five to seven passages. To evaluate insulin uptake and to do so in endothelial cells in which CRP actions via FcγRIIB have been demonstrated and gene silencing can be readily accomplished (24,35), we transfected BAECs with small interfering RNAs using Lipofectamine 2000 (Invitrogen), which were studied 24–48 h later. Double-stranded RNA with sequence 5′-GAAACCAGCCUCUGAA UAAUU-3′ was designed to target the open-reading frame of bovine FcγRIIB (GenBank accession no. NM_174539), and nontargeting siRNA was used as a negative control (D-001810-02-20; ON-TARGETplus Non-targeting siRNA, Dharmacon). Twenty-four hours posttransfection the cells were serum starved for 18 h and incubated with vehicle, CRP (25 μg/mL; EMD Millipore), or CRP plus the NO donor S-nitroso-N-acetylpenicillamine (SNAP) (100 nmol/L; Sigma-Aldrich) for 60 min. Under the same conditions the cells were then incubated with FITC-conjugated insulin (20 nmol/L; Sigma-Aldrich) for 30 min. After washing with PBS the cells were incubated with CAS-Block (Invitrogen) for 60 min and then with primary rabbit anti-FITC antibody (5 μg/mL; Invitrogen) for 60 min followed by fluorecein-conjugated secondary anti-rabbit antibody for 60 min (2 μg/m; Thermo Fisher Scientific). Immunofluoresence was detected by microscopy (×20 magnification; NIKON Eclipse TE2000), and fluorescence intensity (5–6 cells/field

and 6 fields/3 slides/treatment) was quantified using ImageJ software (National Institutes of Health).

To then evaluate insulin transcytosis in endothelial cells in which tight monolayers were readily established, and to concurrently determine whether the processes being studied are operative in human endothelial cells, we performed transcytosis experiments in HAECs as previously described (22). Cells were seeded onto Transwell inserts (6.5 mm diameter, 3 μm pore size; polycarbonate membrane inserts, Sigma-Aldrich) treated with collagen I (BD Bioscience), and transendothelial electrical resistance was monitored 4–5 days later using an epithelial volt-ohmmeter (World Precision Instruments) to confirm the establishment of a confluent monolayer. Vehicle, CRP (25 μg/mL; EMD Millipore), Nω-nitro-L-arginine methyl ester hydrochloride (L-NAME) (20 mmol/L; Sigma Aldrich), or CRP plus SNAP (100 nmol/L; Sigma-Aldrich) was then added together with FITC-insulin (50 nmol/L; Sigma-Aldrich) into the upper chamber, and the cells were incubated for 2 h at 37°C. In separate experiments, vehicle or CRP (25 μg/mL) in the presence of control IgG (10 μg/mL; mouse IgG1, Abcam) or anti-CD32 antibody (10 μg/mL; AT10, Abcam) was placed in the upper chamber along with FITC-insulin. At the end of incubation the FITC-insulin in the lower chamber was quantified using a fluorometer (POLARstar Omega, BMG LABTECH), and the percentage of insulin initially placed in the upper chamber transported to the bottom chamber was calculated. FITC-dextran (M.W. 4000; Sigma-Aldrich) was used to assess paracellular transport.
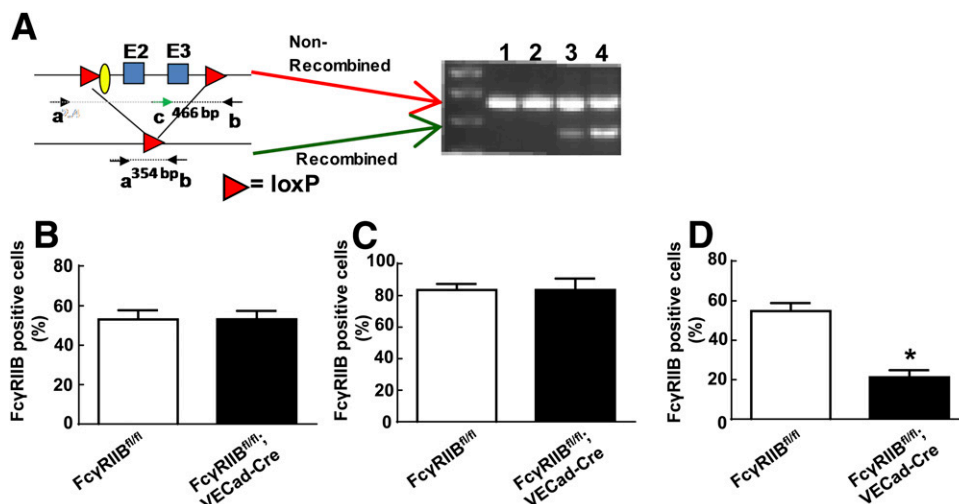
Figure 1—Generation of mice with endothelial-specific deletion of FcγRIIB. *A*: The targeting construct with loxP sites (triangles) flanking exons 2 and 3 (squares) of the mouse FcγRIIB gene is depicted in the upper-left panel. An frt site is also shown (oval). The result of Cre-mediated excision is presented on the lower left, and the location of genotyping primers a, b, and c and the size of resulting PCR products are also shown. On the right are the results of genotyping of aorta from FcγRIIB^fl/fl and FcγRIIB^fl/fl;VECad-Cre mice. In aorta from FcγRIIB^fl/fl mice, the PCR product obtained detected only the nonrecombined allele (466 bp, indicated by red arrow), and this was observed with endothelium-denuded (lane 1) and endothelium-intact (lane 2) aorta. Both nonrecombined and recombined alleles (354 bp PCR product, indicated by green arrow) were detected in aorta from FcγRIIB^fl/fl;VECad-Cre mice, with less signal for the recombined allele evident from endothelium-denuded versus endothelium-intact aorta (lanes 3 and 4, respectively). The less abundant 354 bp PCR product from endothelium-denuded FcγRIIB^fl/fl; VECad-Cre aorta likely arises from residual luminal endothelium or endothelium in vasa vasorum. *B–D*: The expression of FcγRIIB protein in FcγRIIB^fl/fl and FcγRIIB^fl/fl ;VECad-Cre mice was assessed by flow cytometry in splenic B cells (*B*) (n = 4), bone marrow–derived myeloid lineage cells (*C*) (n = 6), and aortic endothelial cells (*D*) (n = 4–6) (*P < 0.05 vs. FcγRIIB^fl/fl). In *B–D*, values are means ± SEM.

Statistical Analysis

Comparisons between two groups were performed by two-tailed Student t tests. Differences between multiple groups were evaluated by one-way ANOVA with Tukey or Sidak post hoc testing. Values shown are mean $\pm$ SEM. Significance was accepted at the 0.05 level of probability.

RESULTS

### Endothelial Deletion of FcγRIIB

To delineate how endothelial FcγRIIB influences glucose homeostasis, we generated mice lacking the receptor specifically in endothelial cells. Endothelial cell–specific excision of the FcγRIIB gene was assessed by genotyping aorta with or without endothelial denudation using the primer sets shown in Fig. 1A. In Cre-expressing mice the predicted 354 base pair (bp) PCR product generated from the recombined allele was evident in aorta, and its abundance was decreased in endothelium-denuded versus endothelium-intact aorta (Fig. 1A, lanes 3 and 4, respectively). The residual signal in endothelium-denuded aorta likely arises from either

remaining luminal endothelium or endothelium in vasa vasorum in the adventitia. The cell-specific deletion of FcγRIIB protein from endothelium was evaluated by flow cytometry. Compared with that in splenic B cells from FcγRIIB$^{fl/fl}$ controls, receptor expression in B cells from FcγRIIB$^{fl/fl}$; VECad-Cre mice was unaltered (Fig. 1B), and bone marrow–derived myeloid lineage cells from the two genotype groups also displayed similar levels of FcγRIIB expression (Fig. 1C). In contrast, there was a 59% decline in FcγRIIB expression in aortic endothelial cells from FcγRIIB$^{fl/fl}$; VECad-Cre mice compared with endothelium from FcγRIIB$^{fl/fl}$ controls (Fig. 1D). Thus, selective diminution of receptor expression was accomplished in endothelium.

Endothelial FcγRIIB Activation and Glucose Intolerance and Insulin Resistance

Metabolic parameters were assessed in FcγRIIB$^{fl/fl}$ controls, FcγRIIB$^{fl/fl}$;TG-CRP mice with elevated CRP and normal endothelial receptor expression, FcγRIIB$^{fl/fl}$;VECad-Cre mice without elevated CRP but deficient in endothelial receptor,
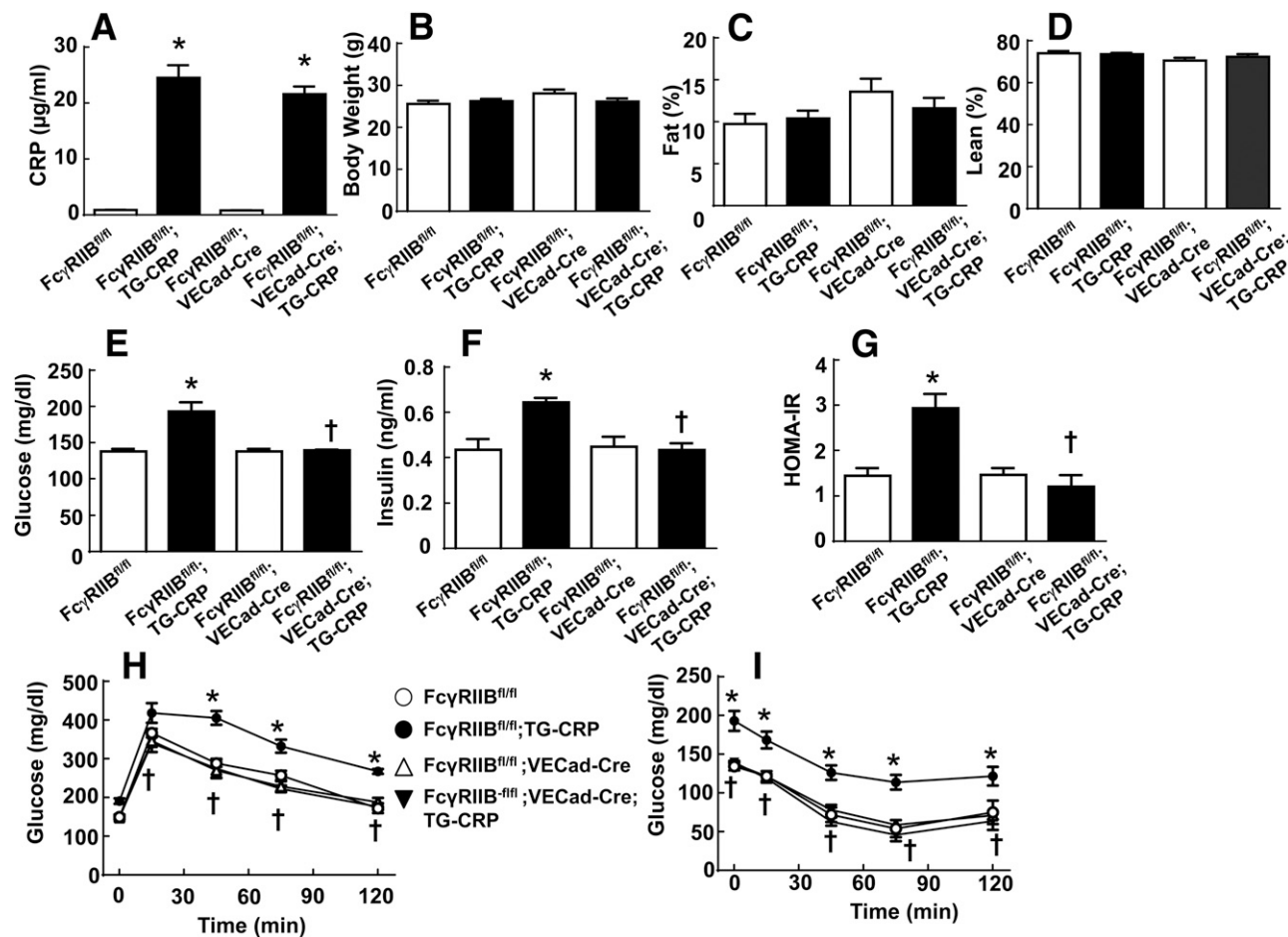
Figure 2—Endothelial FcγRIIB activation by CRP causes glucose intolerance and insulin resistance. A–D: Plasma CRP levels (A), body weight (B), fat mass (C) (% of body weight), and lean body mass (D) (% of body weight) were assessed in male FcγRIIB$^{fl/fl}$, FcγRIIB$^{fl/fl}$;TG-CRP, FcγRIIB$^{fl/fl}$;VECad-Cre, and FcγRIIB$^{fl/fl}$;VECad-Cre;TG-CRP mice at 10 weeks of age ($n = 6$–10) (mean $\pm$ SEM) (*$P < 0.05$ vs. FcγRIIB$^{fl/fl}$). E–I: Male mice (10–13 weeks old) were fasted for 4–6 h, plasma glucose (E) and insulin (F) levels were measured, and HOMA-IR was calculated (G). GTTs (H) and ITTs (I) were performed. In E–I, $n = 6$–8 (mean $\pm$ SEM). *$P < 0.05$ vs. FcγRIIB$^{fl/fl}$, †$P < 0.05$ vs. FcγRIIB$^{fl/fl}$;TG-CRP.

and FcγRIIB^{fl/fl};VECad-Cre:TG-CRP mice with increased circulating CRP and decreased endothelial FcγRIIB. The degree of CRP elevation was similar in FcγRIIB^{fl/fl};TG-CRP and FcγRIIB^{fl/fl};VECad-Cre:TG-CRP mice (Fig. 2A). There were no differences in body weight, fat mass, or lean mass among the four groups (Fig. 2B–D). Consistent with our prior findings in TG-CRP mice (11), FcγRIIB^{fl/fl};TG-CRP mice had elevated fasting glucose and insulin as well as HOMA-IR (Fig. 2E–G). They also showed markedly abnormal GTT and ITT compared with control FcγRIIB^{fl/fl} (Fig. 2H and I). In contrast, mice lacking endothelial FcγRIIB were protected from the effect of CRP on fasting glucose and insulin, HOMA-IR, GTT, and ITT. These findings indicate that endothelial FcγRIIB activation is the primary basis for CRP-induced insulin resistance.

For determination of the basis by which endothelial FcγRIIB^{fl/fl} activation causes insulin resistance, glucose uptake in skeletal muscle was evaluated (11,33). Whereas FcγRIIB^{fl/fl};TG-CRP had decreased glucose uptake compared with control FcγRIIB^{fl/fl} mice, in FcγRIIB^{fl/fl};VECad-Cre;TG-CRP mice the uptake was normalized and was comparable to that of FcγRIIB^{fl/fl};VECad-Cre mice (Fig. 3A). Additional studies were done in FcγRIIB^{fl/fl} and FcγRIIB^{fl/fl};VECad-Cre mice given intraperitoneal injections of vehicle or CRP (250 μg/mouse) 2 h prior to assessment of glucose uptake (5,24). Whereas CRP lowered glucose uptake in control FcγRIIB^{fl/fl} mice, CRP did not do so in FcγRIIB^{fl/fl};VECad-Cre mice (Fig. 3B). Thus, the activation of endothelial FcγRIIB by CRP attenuates skeletal muscle glucose uptake, and a brief elevation in the pentraxin is sufficient to invoke the effect.

Endothelial FcγRIIB Activation and Insulin Delivery and Action in Skeletal Muscle

To next determine how endothelial FcγRIIB activation impacts insulin stimulation of eNOS and insulin action in skeletal muscle, we evaluated insulin-induced eNOS, IR, and Akt phosphorylation in skeletal muscle harvested 5 min after intravenous insulin injection (Fig. 4A–F). In control

FcγRIIB^{fl/fl}, insulin predictably increased the phosphorylation of eNOS, IR, and Akt as indicated by greater phosphorylation at Ser[1176], Tyr[1150/1151], and Ser[473], respectively. In FcγRIIB^{fl/fl}:TG-CRP mice, eNOS phosphorylation in response to insulin was attenuated, and mirroring the observed blunting in skeletal muscle glucose uptake (Fig. 3A), IR and Akt phosphorylation induced by insulin in the skeletal muscle was also diminished. However, in FcγRIIB^{fl/fl}:VECad-Cre mice lacking endothelial FcγRIIB, the enhanced phosphorylation of all these proteins in response to insulin was unaffected by the elevation in CRP.

The basis for the diminished insulin action in skeletal muscle caused by the CRP and endothelial FcγRIIB tandem was then determined. Whereas there was a 392% increase in skeletal muscle insulin content 5 min after bovine insulin injection in FcγRIIB^{fl/fl} controls (Fig. 4G), there was only a 64% increase in muscle insulin in FcγRIIB^{fl/fl};TG-CRP mice. In contrast, FcγRIIB^{fl/fl}VECad-Cre and FcγRIIB^{fl/fl}VECad-Cre;TG-CRP mice showed comparable 296% and 260% increases in insulin in the skeletal muscle after its administration. Collectively these findings indicate that CRP activation of endothelial FcγRIIB attenuates insulin action in skeletal muscle by causing a marked decrease in insulin delivery to the muscle and that this occurs with an associated blunting of eNOS stimulation by insulin.

Endothelial FcγRIIB and Insulin Uptake and Transcytosis

Knowing that insulin uptake by endothelial cells is the rate-limiting step in its transcytosis across the endothelium that delivers it to the skeletal muscle (16–20), we then tested whether FcγRIIB activation by CRP inhibits insulin uptake by cultured endothelial cells in which CRP actions have been demonstrated and small interfering (si)RNA-based silencing is feasible (14,24). BAECs were transfected with control siRNA or siRNA targeting FcγRIIB, and 24 h later the cells were serum starved for 16 h, preincubated
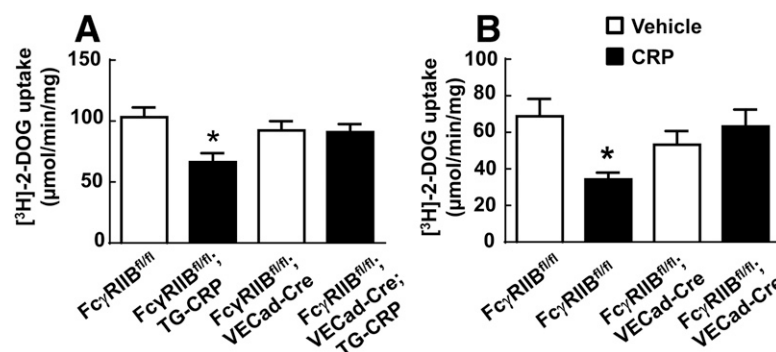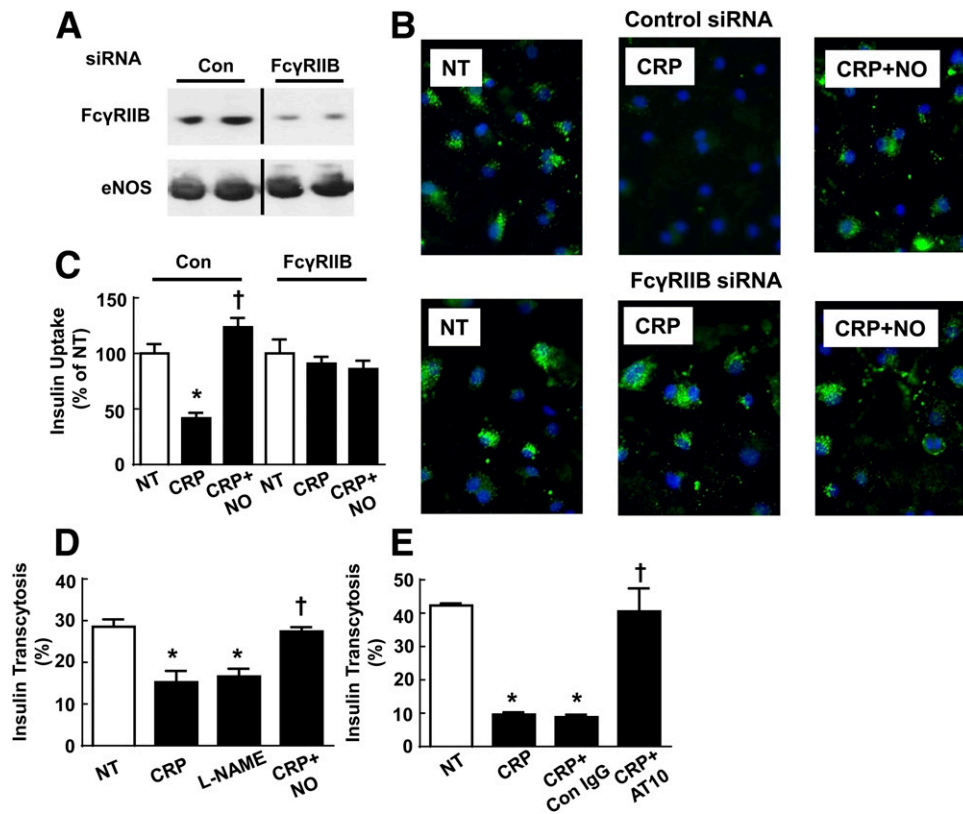

Figure 3—Endothelial FcγRIIB activation by CRP blunts skeletal muscle glucose uptake. A: Male FcγRIIB^{fl/fl}, FcγRIIB^{fl/fl};TG-CRP, FcγRIIB^{fl/fl};VECad-Cre, and FcγRIIB^{fl/fl};VECad-Cre;TG-CRP mice (10–13 weeks old) were injected intraperitoneally with [3H]-2-deoxyglucose ([3H]-2-DOG), and the specific accumulation of [3H]-2-DOG-6-phosphate in skeletal muscle (soleus and gastrocnemius) was determined. Values are mean ± SEM. n = 6. *P < 0.05 vs. FcγRIIB^{fl/fl}. B: Male FcγRIIB^{fl/fl} and FcγRIIB^{fl/fl};VECad-Cre mice (10–13 weeks old) were injected intraperitoneally with human recombinant CRP (200 μg/mouse) or an equal volume of vehicle, and 2 h later they received an intraperitoneal injection of [3H]-2-DOG to assess glucose uptake. Skeletal muscle was isolated, and the accumulation of [3H]-2-DOG-6-phosphate was determined. Values are mean ± SEM, n = 8. *P < 0.05 vs. vehicle.
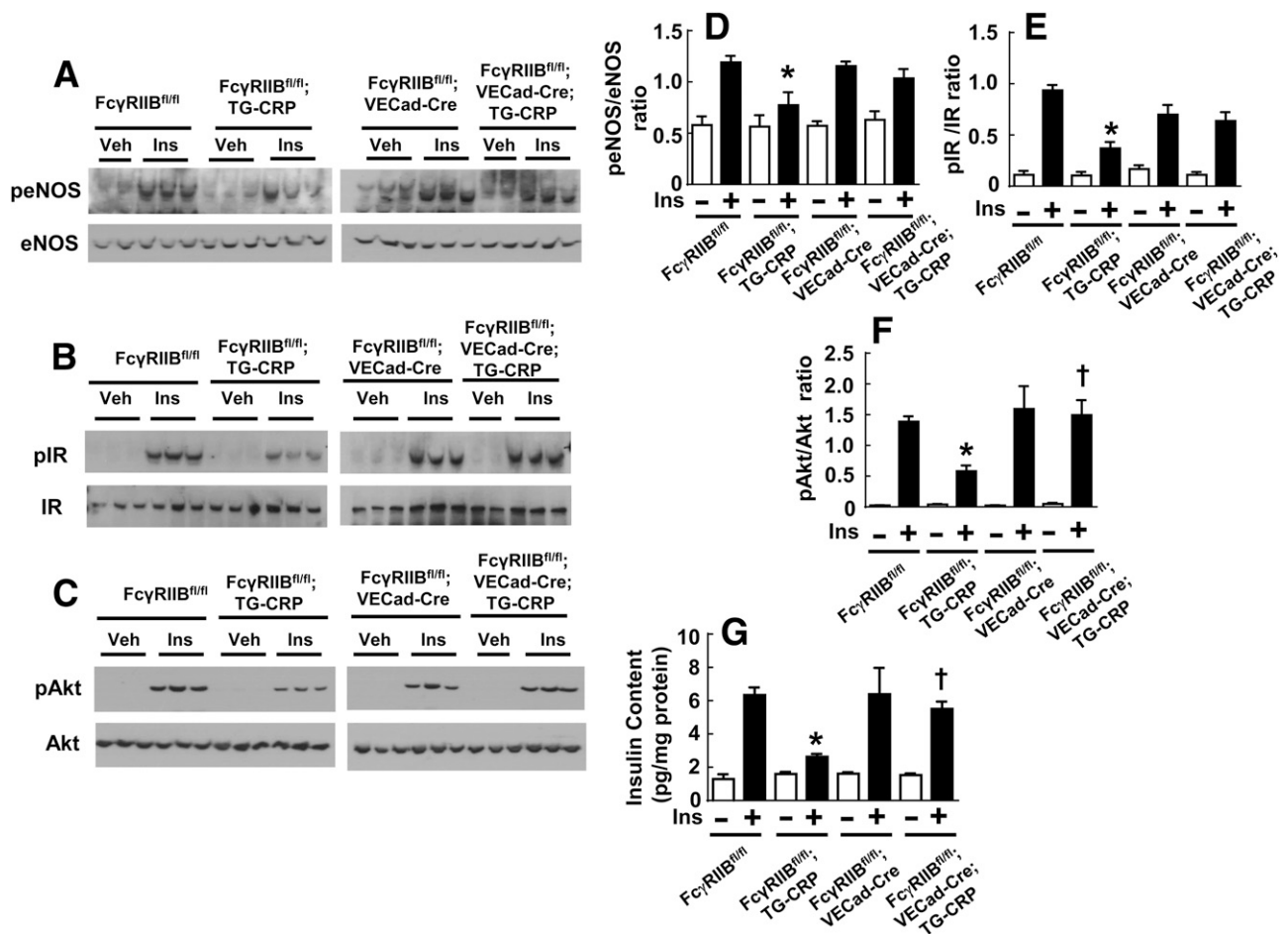
Figure 4—Endothelial FcγRIIB activation by CRP impairs insulin signaling in skeletal muscle by attenuating insulin transport to the tissue. Male FcγRIIB^{fl/fl}, FcγRIIB^{fl/fl};TG-CRP, FcγRIIB^{fl/fl};VECad-Cre, and FcγRIIB^{fl/fl};VECad-Cre;TG-CRP mice (10–13 weeks old) were intravenously injected with vehicle (saline) or insulin (1 unit/kg body wt); 5 min later skeletal muscle was isolated, and lysates were prepared for immunoblotting to detect phosphorylated eNOS (peNOS) at Ser[1176] and total eNOS (A and D), phosphorylated IR (pIR) (β subunit) at Tyr[1150/1151], and total IR (B and E); phosphorylated Akt at Ser[473] (pAkt); and total Akt (C and F) or to quantify insulin content by ELISA (G). A–F: Representative immunoblots for insulin-induced eNOS, IR, and Akt phosphorylation. D–F: Summary data for insulin-induced eNOS, IR, and Akt phosphorylation. G: Insulin concentrations in the skeletal muscle after vehicle or insulin injections. Values are mean ± SEM. n = 5–6. *P < 0.05 vs. FcγRIIB^{fl/fl}, †P < 0.05 vs. FcγRIIB^{fl/fl}:TG-CRP. Ins, insulin; Veh, vehicle.

with vehicle or CRP (25 μg/mL) for 60 min, and then incubated with FITC-conjugated insulin (20 nmol/L) for 30 min. Immunoblotting confirmed a decline in FcγRIIB expression with siRNA knockdown (Fig. 5A). In control siRNA-transfected cells with normal levels of endogenous FcγRIIB, CRP inhibited insulin uptake by 58% (Fig. 5B and C). In contrast, in cells with diminished FcγRIIB expression, CRP did not affect insulin uptake. We previously showed that CRP inhibits eNOS activation by insulin in endothelial cells (14,24), and others have determined that NO promotes insulin uptake into cultured endothelial cells (23). We therefore determined whether impaired insulin uptake upon FcγRIIB activation is due to eNOS antagonism by studying insulin uptake in CRP-treated cells in the absence versus presence of the NO donor SNAP. We found that the supplemental provision of NO prevented the blunting of insulin uptake by CRP activation of FcγRIIB.

The effect of FcγRIIB activation by CRP on endothelial insulin transcytosis was then evaluated in HAECs, in which the required tight monolayers could be established (22). In contrast to control conditions, CRP caused a 47% reduction in insulin transcytosis (Fig. 5D), and an identical decline was observed with eNOS antagonism by L-NAME. Consistent with the findings for insulin uptake, the decrease in insulin transcytosis by CRP was fully prevented by the NO donor SNAP. Transendothelial electrical resistance measurements and assessments of paracellular transport indicated that tight monolayers were maintained under all conditions studied (Supplementary Fig. 2). The involvement of FcγRIIB in CRP inhibition of insulin transcytosis was then assessed using a mouse monoclonal antibody against human FcγRIIB (AT10) (Fig. 5E) (36). Whereas control IgG had no effect, the blocking anti-FcγRIIB antibody fully reversed the inhibitory effect of CRP on insulin transcytosis. Paralleling the in vivo observations

Figure 5—Endothelial cell FcγRIIB activation by CRP inhibits insulin uptake and trancytosis via eNOS antagonism. A–C: Endothelial cells previously transfected with control siRNA (Con) (40 nmol/L) or siRNA targeting FcγRIIB (40 nmol/L) were incubated with vehicle (no treatment [NT]), CRP (25 μg/mL), or CRP + SNAP (NO) (100 nmol/L) for 60 min; FITC-insulin (20 nmol/L) was added for 30 min; and insulin uptake was evaluated by fluorescence microscopy and quantification with ImageJ. A: Immunoblot analyses were performed for FcγRIIB and eNOS to evaluate receptor knockdown (duplicate samples shown). B: Representative immunofluorescence images of insulin accumulation. C: Summary data for insulin uptake. Values are mean ± SEM. n = 6. *P < 0.05 vs. no treatment, †P < 0.05 vs. CRP alone. D: Endothelial cells were grown in transwells to confluency, and vehicle (no treatment), CRP, L-NAME (2 mmol/L), or CRP + SNAP and FITC-insulin (50 nmol/L) were added to the upper chamber. FITC-insulin detected in the lower chamber was measured 2 h later, and the percent of insulin transcytosed was calculated. E: With use of the approach in D, insulin transcytosis was evaluated in cells exposed to vehicle (no treatment), CRP, CRP + control subtype-matched mouse IgG (Con IgG) (10 μg/mL), or CRP + anti-FcγII antibody (AT10) (10 μg/mL). In D and E, values are mean ± SEM. n = 4–7. *P < 0.05 vs. no treatment, †P < 0.05 vs. CRP alone.

for insulin delivery to skeletal muscle (Fig. 4B), these findings reveal that endothelial FcγRIIB activation by CRP attenuates endothelial insulin transcytosis and that this is due to eNOS antagonism.

eNOS Antagonism and CRP-Induced Insulin Resistance

Having demonstrated that the activation of FcγRIIB in cultured endothelial cells has a detrimental impact on insulin transport via the inhibition of eNOS, we next investigated the role of eNOS antagonism in CRP/FcγRIIB-induced insulin resistance in vivo. This was accomplished in eNOS knock-in mice expressing a phosphomimetic, constitutively active form of the enzyme (S1176D) that is not amenable to inhibition by CRP (24,29). S1176D mice were crossed with TG-CRP, and the four resulting study groups had similar body weight and fat and lean body content (Supplementary Fig. 3). The mice expressing eNOS S1176D displayed normal levels of fasting glucose and insulin, and HOMA-IR, GTT, and ITT were similar to those of

wild-type C57BL/6 mice (Fig. 6A–E). Whereas TG-CRP mice expressing wild-type eNOS displayed increases in fasting glucose and insulin, elevated HOMA-IR, and abnormal GTT and ITT, all the parameters were normalized in TG-CRP expressing constitutively active eNOS S1176D. Considered along with the current discovery that endothelial FcγRIIB mediates CRP-induced insulin resistance (Fig. 2), these results indicate that the ligand and endothelial receptor tandem do so in vivo via the inhibition of eNOS.

DISCUSSION

In prior studies we demonstrated that modest elevations in CRP invoke insulin resistance in mice, and the adverse metabolic effects of CRP were negated by the global deletion of the inhibitory Fc receptor FcγRIIB (11). FcγRIIB has numerous classical functions in B cells, T cells, dendritic cells, and monocytes that participate in the regulation of inflammatory responses (1,2,37). Our previous work showed that FcγRIIB is also expressed in endothelial cells,
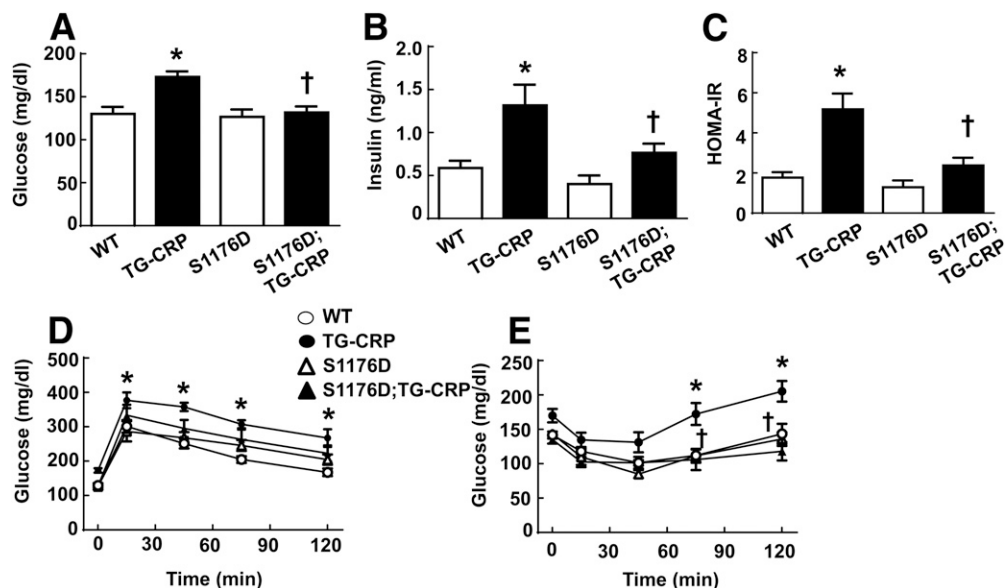
Figure 6—Expression of constitutively active eNOS prevents glucose intolerance and insulin resistance caused by CRP. Male wild-type (WT), TG-CRP, S1176D, and S1176D;TG-CRP mice (10–13 weeks old) were fasted for 4–6 h, and plasma glucose (A) and insulin (B) were measured and HOMA-IR (C) was calculated. GTTs (D) and ITTs (E) were also performed. In A–E, values are mean ± SEM. n = 8–12. *$P < 0.05$ vs. wild type, †$P < 0.05$ vs. TG-CRP.

in which activation of the receptor by CRP triggers signaling that diminishes the activating phosphorylation of eNOS at Ser[1177] to thereby attenuate eNOS enzymatic activity (5). Since FcγRIIB is particularly abundant in B cells and B cells influence insulin sensitivity through multiple mechanisms (12,13), for understanding of how endothelial FcγRIIB impacts glucose homeostasis it was important to segregate possible processes in B cells as well as in other cell types from those occurring in endothelial cells. We therefore created floxed FcγRIIB mice and selectively deleted the receptor from endothelial cells and discovered that mice deficient in the endothelial receptor are fully protected from CRP-induced insulin resistance. Thus, using a genetic strategy we determined that endothelial FcγRIIB has potentially important influence on glucose homeostasis.

In addition to identifying the cell type in which the receptor has the unique ability to have metabolic effects, the processes by which it does so were elucidated in detail (Fig. 7). We previously demonstrated that CRP-induced glucose intolerance involves the attenuation of skeletal muscle glucose disposal (11). In the current work we determined that endothelial FcγRIIB activation by CRP is sufficient to cause the CRP-induced diminution in skeletal muscle glucose disposal in vivo, and there were parallel endothelial FcγRIIB-dependent inhibitory effects of CRP on insulin-induced phosphorylation of skeletal muscle IR and Akt. These findings were related to a marked CRP-induced decline in the delivery of circulating insulin to the skeletal muscle, and the impairment in insulin delivery caused by CRP was fully reversed in mice lacking endothelial FcγRIIB. We previously showed that CRP has an adverse impact on the capacity of insulin to promote

skeletal muscle blood flow (11), and therefore some portion of the blunting in insulin delivery to skeletal muscle by CRP may be related to decreased blood flow. However, an attenuation in the transendothelial transfer of insulin from the circulation to the skeletal muscle myocytes also likely plays an important role because in cultured endothelial cells we discovered that CRP dramatically reduces the uptake of insulin, which is the rate-limiting step in the transcytosis of the hormone across the endothelial cell monolayer (16,18,20,38). In parallel, insulin transcytosis by cultured endothelial cells was markedly decreased by CRP, and mirroring the findings for insulin delivery to the muscle in vivo, the negative impact of CRP on both endothelial insulin uptake and transcytosis in culture was entirely FcγRIIB dependent. Mechanistic linkage between these findings and our prior demonstration of CRP antagonism of eNOS (14,24) then became apparent from the following observations: 1) insulin-induced eNOS phosphorylation in skeletal muscle was blunted by CRP via endothelial FcγRIIB, 2) the provision of exogenous NO rescued normal insulin uptake and transcytosis by cultured endothelial cells despite the presence of CRP, and 3) mice with elevated CRP that express a phosphomimetic, constitutively active form of eNOS (S1177D) displayed normal glucose tolerance and insulin sensitivity. The promotion of insulin uptake in cultured endothelial cells by NO has been reported, and it has been linked to the modulation of PTP1B activity by its nitrosylation (23). However, the present findings reveal for the first time a series of mechanisms that antagonize eNOS and thereby attenuate endothelial insulin uptake and transcytosis in cell culture, and their pathophysiologic relevance is apparent from the parallel observations that were made in vivo.
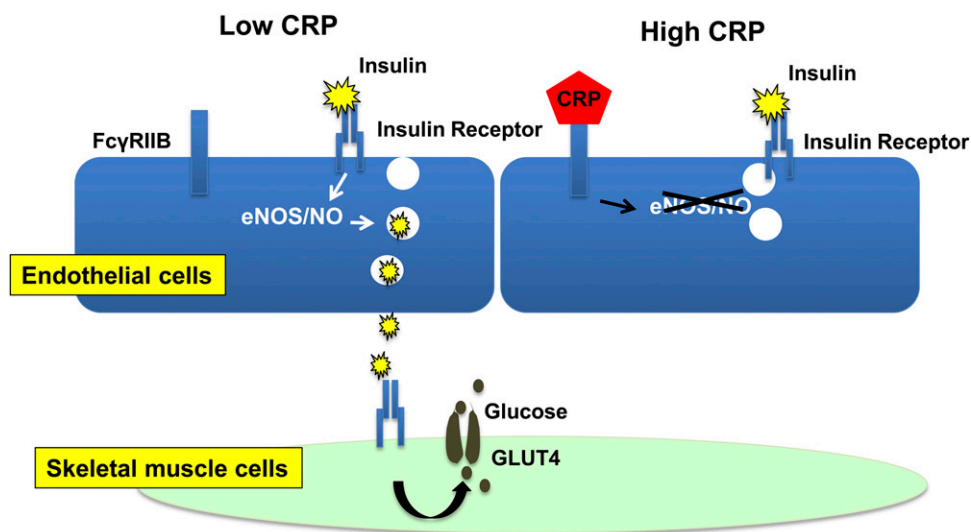
Figure 7—Endothelial FcγRIIB activation by CRP blunts insulin transport to skeletal muscle and thereby attenuates skeletal muscle glucose uptake. Under conditions in which the circulating CRP level is low (shown to left), insulin binding to its receptor on endothelial cells induces eNOS activation and resulting NO production, which promote the transendothelial transport of insulin. Working via the insulin receptor and GLUT4 in the skeletal muscle myocyte, the insulin delivered across the endothelial monolayer promotes glucose uptake. Under conditions in which the CRP level is high (shown to right), CRP binding to FcγRIIB on endothelial cells attenuates insulin-induced eNOS activation, and insulin transcytosis is thereby impaired. As a result, there is diminished insulin-induced skeletal muscle glucose uptake.

At the same time that the current work reveals a specific cell surface receptor in endothelium to be a potent modulator of glucose regulation in vivo, it strengthens the evidence that mechanisms in the endothelium likely have great importance in the pathogenesis of type 2 diabetes. Consistent with the processes revealed in the present studies, eNOS-null mice display insulin resistance and heterozygous eNOS knockout mice become insulin resistant when placed on a high-fat diet, indicating that even a partial loss in these mechanisms has important metabolic consequences under pathologic conditions (39,40). In addition, endothelial cell–specific deletion of insulin receptor substrate (IRS)2, which attenuates insulin signaling and eNOS activation in endothelium, results in decreased skeletal muscle insulin delivery and reduced skeletal muscle glucose disposal (15). In our studies of CRP and endothelial FcγRIIB we observed effects on glucose homeostasis in the fasting state, since there were changes in fasting glucose, insulin, and HOMA-IR, and impact on the fasting state was previously observed with endothelial deletion of IRS1 and IRS2 (15) or the prokineticin receptor-1 (41). Interestingly, in our previous work hyperinsulinemic-euglycemic clamps showed that whereas elevations in CRP cause insulin resistance in the skeletal muscle, they do not induce hepatic insulin resistance (24). In contrast to the skeletal muscle microvasculature, discontinuous endothelium is found in liver sinusoidal vascular beds, and liver sinusoidal endothelium also possesses large fenestrations (42,43). As such, insulin delivery from the circulation to hepatocytes may be passive, whereas the transendothelial transport pathway is critical as a rate-limiting step in the delivery of insulin to skeletal muscle myocytes. The importance of insulin transport to skeletal muscle is particularly apparent in diet-induced obesity, which is a common cause of type 2 diabetes; in mice with diet-induced obesity there is a marked decline in skeletal muscle insulin delivery, and its normalization by an intervention that activates eNOS results in considerable improvement in glucose disposal and glucose tolerance (15). Therefore mechanisms influencing insulin trafficking in endothelium, including possibly the processes revealed here involving FcγRIIB, may emerge as therapeutic targets to pursue in our attempts to prevent or treat type 2 diabetes.

References

1. Ravetch JV, Bolland S. IgG Fc receptors. Annu Rev Immunol 2001;19:275–290

2. Ravetch JV, Lanier LL. Immune inhibitory receptors. Science 2000;290:84–89

3. Lu J, Marnell LL, Marjon KD, Mold C, Du Clos TW, Sun PD. Structural recognition and functional activation of FcgammaR by innate pentraxins. Nature 2008;456:989–992

4. Mold C, Baca R, Du Clos TW. Serum amyloid P component and C-reactive protein opsonize apoptotic cells for phagocytosis through Fcgamma receptors. J Autoimmun 2002;19:147–154

5. Tanigaki K, Sundgren N, Khera A, Vongpatanasin W, Mineo C, Shaul PW. Fc-γ receptors and ligands and cardiovascular disease. Circ Res 2015;116:368–384

6. Bruhns P, Iannascoli B, England P, et al. Specificity and affinity of human Fcgamma receptors and their polymorphic variants for human IgG subclasses. Blood 2009;113:3716–3725

7. Haffner SM. The metabolic syndrome: inflammation, diabetes mellitus, and cardiovascular disease. Am J Cardiol 2006;97:3A–11A

8. Pradhan AD, Cook NR, Buring JE, Manson JE, Ridker PM. C-reactive protein is independently associated with fasting insulin in nondiabetic women. Arterioscler Thromb Vasc Biol 2003;23:650–655

9. Pradhan AD, Manson JE, Rifai N, Buring JE, Ridker PM. C-reactive protein, interleukin 6, and risk of developing type 2 diabetes mellitus. JAMA 2001;286: 327–334

10. Yudkin JS, Stehouwer CD, Emeis JJ, Coppack SW. C-reactive protein in healthy subjects: associations with obesity, insulin resistance, and endothelial dysfunction: a potential role for cytokines originating from adipose tissue? Arterioscler Thromb Vasc Biol 1999;19:972–978

11. Tanigaki K, Vongpatanasin W, Barrera JA, et al. C-reactive protein causes insulin resistance in mice through Fc-γ receptor IIB-mediated inhibition of skeletal muscle glucose delivery. Diabetes 2013;62:721–731

12. Winer DA, Winer S, Shen L, et al. B cells promote insulin resistance through modulation of T cells and production of pathogenic IgG antibodies. Nat Med 2011; 17:610–617

13. Shen L, Chng MH, Alonso MN, Yuan R, Winer DA, Engleman EG. B-1a lymphocytes attenuate insulin resistance. Diabetes 2015;64:593–603

14. Mineo C, Gormley AK, Yuhanna IS, et al. FcgammaRIIB mediates C-reactive protein inhibition of endothelial NO synthase. Circ Res 2005;97:1124–1131

15. Kubota T, Kubota N, Kumagai H, et al. Impaired insulin signaling in endothelial cells reduces insulin-induced glucose uptake by skeletal muscle. Cell Metab 2011;13:294–307

16. Barrett EJ, Liu Z. The endothelial cell: an "early responder" in the development of insulin resistance. Rev Endocr Metab Disord 2013;14:21–27

17. Barrett EJ, Eggleston EM, Inyard AC, et al. The vascular actions of insulin control its delivery to muscle and regulate the rate-limiting step in skeletal muscle insulin action. Diabetologia 2009;52:752–764

18. Chiu JD, Richey JM, Harrison LN, et al. Direct administration of insulin into skeletal muscle reveals that the transport of insulin across the capillary endothelium limits the time course of insulin to activate glucose disposal. Diabetes 2008;57:828–835

19. Freidenberg GR, Suter SL, Henry RR, Reichart D, Olefsky JM. In vivo stimulation of the insulin receptor kinase in human skeletal muscle. Correlation with insulin-stimulated glucose disposal during euglycemic clamp studies. J Clin Invest 1991;87:2222–2229

20. Miles PD, Levisetti M, Reichart D, Khoursheed M, Moossa AR, Olefsky JM. Kinetics of insulin action in vivo. Identification of rate-limiting steps. Diabetes 1995;44:947–953

21. Wang H, Wang AX, Liu Z, Barrett EJ. Insulin signaling stimulates insulin transport by bovine aortic endothelial cells. Diabetes 2008;57:540–547

22. Wang H, Liu Z, Li G, Barrett EJ. The vascular endothelial cell mediates insulin transport into skeletal muscle. Am J Physiol Endocrinol Metab 2006;291: E323–E332

23. Wang H, Wang AX, Aylor K, Barrett EJ. Nitric oxide directly promotes vascular endothelial insulin transport. Diabetes 2013;62:4030–4042

24. Tanigaki K, Mineo C, Yuhanna IS, et al. C-reactive protein inhibits insulin activation of endothelial nitric oxide synthase via the immunoreceptor tyrosine-based inhibition motif of FcgammaRIIB and SHIP-1. Circ Res 2009;104:1275–1282

25. Alva JA, Zovein AC, Monvoisin A, et al. VE-Cadherin-Cre-recombinase transgenic mouse: a tool for lineage analysis and gene deletion in endothelial cells. Dev Dyn 2006;235:759–767

26. Sundgren NC, Zhu W, Yuhanna IS, et al. Coupling of Fc-γ receptor I to Fc-γ receptor IIb by SRC kinase mediates C-reactive protein impairment of endothelial function. Circ Res 2011;109:1132–1140

27. Vongpatanasin W, Thomas GD, Schwartz R, et al. C-reactive protein causes downregulation of vascular angiotensin subtype 2 receptors and systolic hypertension in mice. Circulation 2007;115:1020–1028

28. Atochin DN, Huang PL. Endothelial nitric oxide synthase transgenic models of endothelial dysfunction. Pflugers Arch 2010;460:965–974

29. Atochin DN, Wang A, Liu VW, et al. The phosphorylation state of eNOS modulates vascular reactivity and outcome of cerebral ischemia in vivo. J Clin Invest 2007;117:1961–1967

30. Kobayashi M, Inoue K, Warabi E, Minami T, Kodama T. A simple method of isolating mouse aortic endothelial cells. J Atheroscler Thromb 2005;12:138–142

31. Tanigaki K, Vongpatanasin W, Barrera JA, et al. C-reactive protein causes insulin resistance in mice through Fc-γ receptor IIB-mediated inhibition of skeletal muscle glucose delivery. Diabetes 2013;62:721–731

32. Matthews DR, Hosker JP, Rudenski AS, Naylor BA, Treacher DF, Turner RC. Homeostasis model assessment: insulin resistance and beta-cell function from fasting plasma glucose and insulin concentrations in man. Diabetologia 1985;28: 412–419

33. Zisman A, Peroni OD, Abel ED, et al. Targeted disruption of the glucose transporter 4 selectively in muscle causes insulin resistance and glucose intolerance. Nat Med 2000;6:924–928

34. Shao J, Yamashita H, Qiao L, Friedman JE. Decreased Akt kinase activity and insulin resistance in C57BL/KsJ-Leprdb/db mice. J Endocrinol 2000;167: 107–115

35. Ulrich V, Gelber SE, Vukelic M, et al. ApoE Receptor 2 Mediation of Trophoblast Dysfunction and Pregnancy Complications Induced by Antiphospholipid Antibodies in Mice. Arthritis Rheumatol 2016;68:730–739

36. Devaraj S, Davis B, Simon SI, Jialal I. CRP promotes monocyte-endothelial cell adhesion via Fcgamma receptors in human aortic endothelial cells under static and shear flow conditions. Am J Physiol Heart Circ Physiol 2006;291: H1170–H1176

37. Marnell L, Mold C, Du Clos TW. C-reactive protein: ligands, receptors and role in inflammation. Clin Immunol 2005;117:104–111

38. Vincent MA, Clerk LH, Rattigan S, Clark MG, Barrett EJ. Active role for the vasculature in the delivery of insulin to skeletal muscle. Clin Exp Pharmacol Physiol 2005;32:302–307

39. Duplain H, Burcelin R, Sartori C, et al. Insulin resistance, hyperlipidemia, and hypertension in mice lacking endothelial nitric oxide synthase. Circulation 2001;104:342–345

40. Shankar RR, Wu Y, Shen HQ, Zhu JS, Baron AD. Mice with gene disruption of both endothelial and neuronal nitric oxide synthase exhibit insulin resistance. Diabetes 2000;49:684–687

41. Dormishian M, Turkeri G, Urayama K, et al. Prokineticin receptor-1 is a new regulator of endothelial insulin uptake and capillary formation to control insulin sensitivity and cardiovascular and kidney functions. J Am Heart Assoc 2013;2: e000411

42. Aird WC. Phenotypic heterogeneity of the endothelium: I. Structure, function, and mechanisms. Circ Res 2007;100:158–173

43. Aird WC. Phenotypic heterogeneity of the endothelium: II. Representative vascular beds. Circ Res 2007;100:174–190